Journal of Steroid Biochemistry & Molecular Biology 127 (2011) 238–247

Contents lists available at SciVerse ScienceDirect

Journal of Steroid Biochemistry and Molecular Biology

journal homepage: www.elsevier.com/locate/jsbmb

Cytochrome b_5 augments 3β-hydroxysteroid dehydrogenase/Δ^5-Δ^4 isomerase activity

Pierre Goosen, Karl-Heinz Storbeck, Amanda C. Swart, Riaan Conradie, Pieter Swart*

Department of Biochemistry, University of Stellenbosch, Stellenbosch 7602, South Africa

ARTICLE INFO

Article history:
Received 30 July 2011
Received in revised form 1 September 2011
Accepted 4 September 2011

Keywords:
Cytochrome-b_5
3β-Hydroxysteroid dehydrogenase/isomerase
Cytochrome P450 17α-hydroxylase/17,20 lyase
Adrenal steroidogenesis

ABSTRACT

During adrenal steroidogenesis the competition between 3β-hydroxysteroid dehydrogenase/Δ^5-Δ^4 isomerase (3βHSD) and cytochrome P450 17α-hydroxylase/17,20 lyase (CYP17A1) for Δ^5 steroid intermediates greatly influences steroidogenic output. Cytochrome-b_5 (Cyt-b_5), a small electron transfer hemoprotein, known to augment the lyase activity of CYP17A1, has been shown to alter the steroidogenic outcome of this competition. In this study, the influence of Cyt-b_5 on 3βHSD activity was investigated. In COS-1 cells, Cyt-b_5 was shown to significantly increase the activity of both caprine and ovine 3βHSD towards pregnenolone, 17-OH pregnenolone and dehydroepiandrosterone in a substrate and species specific manner. Furthermore, kinetic studies revealed Cyt-b_5 to have no influence on the K_m values while significantly increasing the V_{max} values of ovine 3βHSD for all its respective substrates. In addition, the activity of ovine 3βHSD in microsomal preparations was significantly influenced by the addition of either purified Cyt-b_5 or anti-Cyt-b_5 IgG. The results presented in this study indicate that Cyt-b_5 augments 3βHSD activity and represents the first documentation of such augmentation in any species.

1. Introduction

Hydroxysteroid dehydrogenases play pivotal roles in the biosynthesis and inactivation of steroid hormones. In steroidogenic tissue, members in this class catalyze the biosynthesis of steroid hormones while they convert potent steroid hormones to inactive metabolites in peripheral tissue [1].

During the biosynthesis of steroid hormones in the adrenal cortex, 3β-hydroxysteroid dehydrogenase/Δ^5-Δ^4 isomerase (3βHSD) plays a central role in the production of mineralocorticoids, glucocorticoids and C19 steroids [2]. 3βHSD catalyzes the conversion of the Δ^5 steroids, pregnenolone (PREG), 17-hydroxypregnenolone (17-OHPREG) and dehydroepiandrosterone (DHEA) to the corresponding Δ^4 steroids, progesterone (PROG), 17-hydroxyprogesterone (17-OHPROG) and androstenedione (A4) through a sequential two-step reaction [3,4]. In the first dehydrogenation reaction, NAD^+ is reduced to NADH with the formation of a $\Delta^{5\text{-}3}$ keto steroid intermediate which, together with NADH, remains bound to the enzyme. The bound NADH induces conformational changes in the enzyme resulting in the isomerization of the bound intermediate to form the corresponding Δ^4 steroid product [4,5]. According to the model proposed by Thomas et al. [4], the dehydrogenase and isomerase domains of the enzyme are linked by a shared coenzyme domain that functions as both the binding site for NAD^+ during the dehydrogenase reaction and for the reduced NADH, with the latter subsequently acting as an allosteric activator of the isomerase reaction.

During the synthesis of steroid hormones, 3βHSD competes with cytochrome P450 17α-hydroxylase/17,20 lyase (CYP17A1) for Δ^5-steroid intermediates. CYP17A1 catalyzes two distinct reactions, the 17α-hydroxylation of PREG and PROG yielding 17-OHPREG and 17-OHPROG, and the subsequent 17,20 lyase reaction resulting in the cleavage of the C17,20 bond yielding DHEA and A4, respectively [6–8]. Due to the competition between 3βHSD and CYP17A1 for PREG and 17-OHPREG, the ratio of the enzyme activities and substrate specificities are crucial in determining the flux of steroid intermediates through the steroidogenic pathways [9–12]. This competition is significantly altered by cytochrome-b_5 (Cyt-b_5), which selectively stimulates the lyase activity of CYP17A1 resulting in a substantial increase in C19 steroid production [13,14].

Cyt-b_5 is a small ubiquitous electron-transfer hemoprotein. The microsomal form of Cyt-b_5 expressed in steroidogenic tissue consists of two domains: a larger globular head domain, which contains the heme moiety, and a smaller hydrophobic membrane anchoring tail domain. The two domains are connected by a proline containing hinge region [15,16]. To date, studies investigating the influence of Cyt-b_5 on steroidogenesis have focused primarily on

Abbreviations: *apo*-b_5, wild type cytochrome-b_5 void of heme; POR, P450 oxidoreductase; CFP, cyan fluorescent protein; YFP, yellow fluorescent protein; *holo*-b_5, wild type cytochrome-b_5; trunc-b_5, truncated wild type cytochrome-b_5.

* Corresponding author. Tel.: +27 21 808 5865; fax: +27 21 808 5863.
E-mail addresses: pswart@sun.ac.za, butrosblack@gmail.com (P. Swart).

0960-0760/$ – see front matter © 2011 Elsevier Ltd. All rights reserved.
doi:10.1016/j.jsbmb.2011.09.001

the stimulation of CYP17A1 lyase activity as none of the other steroidogenic cytochromes P450 have been shown to be influenced by Cyt-b_5. In addition, no data is available describing the influence of Cyt-b_5 on 3βHSD.

Since the augmentation of 3βHSD activity by Cyt-b_5 would contribute towards the alteration in steroidogenic output as is observed for CYP17A1 in the presence of Cyt-b_5, the potential influence of Cyt-b_5 on 3βHSD activity was investigated. In this study, Cyt-b_5 was co-expressed with both caprine and ovine 3βHSD in nonsteroidogenic COS-1 cells and the catalytic activities towards PREG, 17-OHPREG and DHEA assayed in the absence of other steroidogenic enzymes. In addition, ovine adrenal microsomes were prepared and 3βHSD activity assayed in the presence and absence of purified Cyt-b_5 and anti-Cyt-b_5 IgG.

2. Materials and methods

2.1. Materials

Plasmid vectors, Gene Tailor™ site-directed mutagenesis system and MultiSite Gateway® Pro cloning system were purchased from Invitrogen Life Technologies (Carlsbad, CA, USA). Primers were purchased from Integrated DNA Technologies (Coralville, IA, USA). Nucleobond® AX plasmid purification kits were supplied by Macherey-Nagel (Duren, Germany) and Wizard® *Plus* SV Minipreps DNA Purification kits were purchased from Promega Biotech (Madison, WI, USA). COS-1 cells were obtained from the American Type Tissue Culture Collection (Manassas, VA, USA). Mirus *Trans*IT®-LT1 transfection reagent was purchased from Mirus Bio Corporation (Madison, WI, USA). Fetal calf serum and bacterial culture medium were purchased from Highveld Biological (Lyndhurst, SA) and Difco Laboratories (Detroit, MI, USA), respectively. Penicillin–streptomycin, trypsin–EDTA and Dulbecco's phosphate buffered saline (PBS) were purchased from Gibco BRL (Gaithersburg, MD, USA). [1,2,6,7-^{3}H]-DHEA and [7-^{3}H]-PREG were purchased from Perkin Elmer Life Sciences (Boston, MA, USA). PREG, 17-OHPREG, DHEA, Dulbecco's modified Eagle's medium (DMEM) were supplied by Sigma Chemical Co. (St. Louis, MO, USA). A bicinchoninic acid (BCA) protein assay kit was purchased from Pierce (Rockford, IL, USA). All other chemicals were of the highest quality and obtained from reputable scientific supply houses.

2.2. Preparation of plasmid constructs

Angora goat/caprine (GenBank accession no. EF524065), ovine 3βHSD (GenBank accession no. FJ007375) and caprine Cyt-b_5 (GenBank accession no. EF524066) were previously cloned into the pcDNA3.2/V5/GW/D-TOPO® vector (Invitrogen Life Technologies, Carlsbad, CA, USA) as described by Storbeck et al. [17] and Goosen et al. [18].

Apo- (wild type Cyt-b_5 void of heme) and trunc- (truncated wild type Cyt-b_5) forms of caprine Cyt-b_5 were prepared using the Gene Tailor™ site-directed mutagenesis system (Invitrogen Life Technologies, Carlsbad, CA, USA) according to the manufacturer's instructions. The primers used to create *apo*-b_5, which contained a H68A mutation [19], were: sense primer, 5′-AAA ACT TTG AGG ACG TTG GAG CCT CTA CAG ATG CT-3′; antisense primer, 5′-TCC AAC GTC CTC AAA GTT TTC AGT GGC ATC-3′.

Trunc-b_5 was created by inserting a stop codon at position 270 terminating translation of 45 amino acid residues at the C-terminus of *holo*-b_5 (wild type Cyt-b_5). The primers used were: sense primer, 5′-GCT GCA CCC GGA TGA CAG ATG AAA GAT AAC CA-3′; antisense primer, 5′-ATC TGT CAT CCG GGT GCA GCT CCC CAA TGA-3′. The mutations were subsequently confirmed by direct DNA sequence analysis using an ABI Prism 3100 Genetic Analyzer (Applied Biosystems, Johannesburg, RSA).

Ovine 3βHSD-CFP (Cyan Fluorescent Protein) and *holo*-b_5-YFP (Yellow Fluorescent Protein) plasmid constructs were prepared using the MultiSite Gateway® Pro cloning system (Invitrogen Life Technologies, Carlsbad, CA, USA), according to the manufacturer's instructions. The primers used to amplify ovine 3βHSD from the pcDNA3.2/V5/GW/D-TOPO® vector and CFP from the Cer-5-Ven vector during the construction of the 3βHSD-CFP chimeric construct were: sense primer 3βHSD-attB1, 5′-GGG GAC AAG TTT GTA CAA AAA AGC AGG CTA TGG CGG GCT GGA GCT GCC TG-3′; antisense primer 3βHSD-attB5r, 5′-GGG GAC AAC TTT TGT ATA CAA AGT TGT ATG AAT TTT GGT TTT CAG GGT-3′ and sense primer CFP-attB5, 5′-GGG GAC AAC TTT GTA TAC AAA AGT TGC GAT GGT GAG CAA GGG CGA GG-3′; antisense primer CFP-attB2r, 5′-GGG GAC CAC TTT GTA CAA GAA AGC TGG GTA TCC GGA CTT GTA CAG CTC-3′. The primers used to amplify *holo*-b_5 from the pcDNA3.2/V5/GW/D-TOPO® vector and YFP from the Cer-5-Ven vector during the construction of the *holo*-b_5-YFP chimeric construct were: sense primer *holo*-b_5-attB5, 5′-GGG GAC AAC TTT GTA TAC AAA AGT TGC GTC GCT GAG TTA AGA AAT GGC C-3′; antisense primer *holo*-b_5-attB2r, 5′-GGG GAC CAC TTT GTA CAA GAA AGC TGG GTA CTC CCT GGA CCA AAG CAG-3′ and sense primer YFP-attB1, 5′-GGG GAC AAG TTT GTA CAA AAA AGC AGG CTA GAT CCG CTA GCG CTA C-3′; antisense primer YFP-attB5r, 5′-GGG GAC AAC TTT TGT ATA CAA AGT TGT TCC GGA CTT GTA CAG CTC-3′.

2.3. Caprine and ovine 3βHSD enzyme activity assay in transiently transfected COS-1 cells

COS-1 cells were grown at 37 °C and 5% CO_2 in Dulbecco's modified Eagle's medium (DMEM) supplemented with 10% fetal calf serum, 1% penicillin–streptomycin and 0.12% $NaHCO_3$. Cells were plated into 12-well plates with each well containing 1.0×10^5 cells in 1 ml, 24 h prior to transfection. The cells were transiently cotransfected with DNA plasmid constructs, 1 μg, using *Trans*IT®-LT1 transfection reagent (Mirus), according to manufacturer's instructions.

PREG, 17-OHPREG and DHEA metabolism were assayed in cells cotransfected with either caprine or ovine 3βHSD (0.5 μg) and *holo*-b_5 (0.5 μg). Control transfection reactions were performed using either caprine or ovine 3βHSD (0.5 μg) and the mammalian expression vector pCI-neo (0.5 μg) (Promega, Madison, WI, USA) which contained no DNA insert. PREG metabolism was also assayed in cells in which ovine 3βHSD was cotransfected with equal amounts of either *holo*-b_5, trunc-b_5, pCI-neo or human 11β-hydroxysteroid dehydrogenase type 2 (11βHSD2) [20]. The influence of Cyt-b_5 electron transfer on PREG metabolism by 3βHSD was assayed in cells cotransfected with either *holo*-b_5 or *apo*-b_5 (0.2–0.8 μg) and ovine 3βHSD (0.2 μg) in ratios ranging from 1:1 to 1:4 with pCI-neo added to keep the amount of DNA constant.

Enzyme activity was assayed after 72 h by adding appropriate steroid substrates – PREG and [^{3}H]PREG; 17-OHPREG; DHEA and [^{3}H]DHEA. At specific time intervals aliquots were removed from the assay mixtures, 50 μl from the PREG and DHEA conversion assays and 500 μl from the 17-OHPREG assay. The steroid metabolites were subsequently extracted by liquid–liquid extraction using a 10:1 volume of dichloromethane to incubation medium. The samples were vortexed for 15 min and centrifuged at 500 × *g* for 5 min. The water phase was aspirated off, and the dichloromethane phase transferred to a clean test tube and dried under N_2. The dried steroid residue was redissolved in 120 μl methanol prior to HPLC or UPLC–MS analysis. After completion of each experiment, the cells were washed and collected in phosphate buffer (0.1 M, pH 7.4). The cells were homogenized with a small glass homogenizer and the total protein content of the homogenate was determined using

the Pierce BCA™ protein assay kit according to the manufacturer's instructions.

2.4. Expression and visualization of 3βHSD-CFP and holo-b_5-YFP fusion proteins in transiently transfected COS-1 cells

COS-1 cells were grown as described in Section 2.3. Cells were plated into 6-well plates (2.0×10^5 cells/well) with each well containing a small glass cover slip, 24 h prior to transfection. The cells were transiently cotransfected with DNA plasmid constructs, 2 μg, using *Trans*IT®-LT1 transfection reagent (Mirus), according to manufacturer's instructions. The level of fluorescence of each fusion protein was investigated in cells cotransfected with either 3βHSD-CFP (1 μg) and *holo*-b_5-YFP (1 μg) or 3βHSD-CFP (0.4 μg) and *holo*-b_5-YFP (0.4–1.6 μg) in ratios ranging from 1:1 to 1:4 with pCI-neo added to keep the amount of DNA constant.

Forty-eight hours post-transfection the cells were washed with methanol (−20 °C) and fixed by incubation in methanol (1 ml) for 20 min at −20 °C. Following fixation the cells were washed three times with phosphate buffer containing 0.2% bovine serum albumin and mounted on individual object slides.

The cells were subsequently analyzed for fluorescence using an Olympus CellR system attached to an IX 81 inverted fluorescence microscope (Olympus Corp.) equipped with an F-view-II cooled CCD camera (Soft Imaging Systems). The light source was a 150 W Xenon lamp, part of an MT20 excitation system. Cells were observed with a 60× oil immersion objective and the Cell® imaging software was used for image acquisition and analysis. The YFP filter set excited at S500/20x (Chroma) and emission was detected at S535/30m, whereas the CFP filter set excited at S430/25x and emission was detected at S470/30m.

2.5. Preparation of adrenal microsomes

Ovine adrenals were obtained at a local abattoir and immediately stored on ice. All subsequent procedures were performed at 4 °C. Microsomes were prepared according to the differential centrifugation method of Yang and Cederbaum [21]. Briefly, following the removal of the capsule and excess fat, fresh adrenals were washed with a 15 mM KCl solution. The adrenal tissue was homogenized in three volumes 10 mM Tris–HCl buffer (pH 7.4) containing 1.0 mM EDTA and 0.25 M sucrose and centrifuged for 15 min at 500 × *g*. The supernatant was centrifuged at 12 000 × *g* for 15 min. A 50% (w/v) PEG 8000 solution was added while stirring to the postmitochondrial supernatant to a final concentration of 8.5%. The mixture was stirred for 10 min and centrifuged at 13 000 × *g* for 20 min. The microsomal pellet was homogenized in 200 ml 10 mM Tris–HCl buffer (pH 7.4) containing 150 mM KCl and 1.0 mM EDTA. A 50% (w/v) PEG 8000 solution was again added to the suspension to a final concentration of 8.5% and stirred for 10 min at 4 °C, followed by centrifugation at 13 000 × *g* for 20 min. This procedure was repeated twice until the supernatant was clear. The final microsomal pellet was re-suspended in 10 mM Tris–HCl buffer (pH 7.4) containing 1.0 mM EDTA and 0.25 mM sucrose and stored at −80 °C. The total protein content of the preparation was determined using a Pierce BCA™ protein assay kit according to manufacturer's instructions. Finally, the P450 and Cyt-b_5 content of the microsomal preparation was determined spectrophotometrically, as previously described [22,23].

2.6. Isolation and purification of ovine Cyt-b_5

Ovine liver was obtained at a local abattoir and immediately stored on ice. Liver microsomes were prepared according to the differential centrifugation method of Yang and Cederbaum [21]. Cyt-b_5 was subsequently purified from the microsomal preparation as described by Swart et al. [10]. Briefly, the microsomal fraction was loaded onto a DEAE-cellulose column (3.2 × 20 cm) equilibrated with 80 mM Tris acetate, 1 mM EDTA, 2% Triton X-100, pH 8.1. Cyt-b_5 reductase was eluted with 0.1 M Tris acetate, 1 mM EDTA, 2% Triton X-100, pH 8.1 after which a linear gradient from 0 to 50 mM NaSCN was run over 3 bed volumes in 10 mM Tris acetate, 1 mM EDTA, 0.1% deoxycholate, 0.2% Triton X-100, pH 8.1. Cyt-b_5 was subsequently eluted with 90 mM NaSCN in 10 mM Tris acetate buffer and dialyzed overnight against ten volumes 10 mM Tris acetate buffer. Following dialysis, the Cyt-b_5 solution was applied to a DEAE-cellulose column (2 × 20 cm) equilibrated with 10 mM Tris acetate, 1 mM EDTA, 0.2% Triton X-100, 0.05% deoxycholate, pH 8.1. A linear NaSCN gradient from 0 to 50 mM in equilibration buffer was followed by a linear NaSCN gradient from 50 mM to 90 mM to elute Cyt-b_5. The Cyt-b_5 solution was subsequently dialyzed overnight against 10 volumes 10 mM Tris acetate, 0.1 mM EDTA, pH 8.1. Following dialysis, the solution was applied to a DEAE-cellulose column (1 × 5 cm) equilibrated with 10 mM Tris acetate, 0.1 mM EDTA, pH 8.1. Finally, Cyt-b_5 was eluted with 10 mM Tris acetate, 0.1 mM EDTA, 0.25% sodium deoxycholate, pH 8.1 and dialyzed overnight against ten volumes of elution buffer and the resulting Cyt-b_5 solution stored at −80 °C. The Cyt-b_5 content was determined spectrophotometrically as previously described [23]. The total protein content of the solution was determined using a Pierce BCA™ protein assay kit according to manufacturer's instructions.

2.7. Microsomal 3βHSD enzyme activity assay

3βHSD enzyme activity was assayed in ovine adrenal microsomes as previously described [10]. Briefly, incubations were performed in a water bath at 37 °C in a total volume of 500 μl. The reaction mixture contained microsomal preparation (0.35 μM P450) and was carried out in 50 mM Tris buffer containing 1% (m/v) bovine serum albumin and 50 mM NaCl. Following a 5 min pre-incubation of the reaction mixture at 37 °C with either PREG and [^{3}H]PREG; 17-OHPREG or DHEA and [^{3}H]DHEA as substrates, the reaction was initiated by the addition of 0.5 mM NAD^+. Aliquots (50 μl) were removed from the assay mixture at specific time intervals and the steroid metabolites subsequently extracted by liquid–liquid extraction as described in Section 2.3.

For the inhibition of 3βHSD activity, trilostane (10 μM) was added to the microsomal preparation and incubated on ice for 15 min prior to pre-incubation. For the inhibition of endogenous Cyt-b_5, the microsomal preparation was incubated on ice for 1 h prior to pre-incubation with purified anti-ovine Cyt-b_5 IgG (200 μl), previously raised in our laboratory [10]. The activation of 3βHSD activity by Cyt-b_5 was assessed by adding increasing amounts of purified Cyt-b_5 to obtain a range of ratios (endogenous Cyt-b_5:added Cyt-b_5) in the microsomal preparation. A 15 min incubation period was carried out on ice prior to pre-incubation.

2.8. Separation and quantification of steroids

High performance liquid chromatography was performed on a SpectraSYSTEM P4000 high performance liquid chromatograph (Thermo Separation™ products, San Jose, CA, USA) coupled to a SpectraSYSTEM AS3000 automatic injector (Thermo Separation™ products, San Jose, CA, USA) and a Flo-One liquid scintillation spectrophotometer (Radiomatic, Tampa, FL, USA). The substrates, PREG and DHEA, and their respective steroid metabolites were separated using a Phenomex® C_{12} column at a flow rate of 1 ml min^{-1}. The ratio of scintillant to column element was 3:1. For the separation of PREG from PROG the mobile phase consisted of solvent A (methanol/water: 75%/25%) and solvent B (100% methanol). Steroids were eluted for 2 min with solvent A, followed by a linear gradient from 100% A to 100% B in 9 min and an isocratic elution

with solvent B for 2 min. DHEA and A4 were eluted with solvent A (methanol/water: 65%/35%) for 15 min, followed by a linear gradient from 100% A to 100% B (100% methanol) in 2 min and an isocratic elution with solvent B for 2 min. The injection volume of the samples was 90 μl.

17-OHPREG and 17-OHPROG were separated by UPLC (ACQUITY UPLC, Waters, Milford, MA, USA) using a Waters UPLC BEH C_{18} column (2.1 × 50 mm, 1.7 μm) at 50 °C and a flow rate of 0.4 ml min^{-1} as previously described. An API Quattro Micro tandem mass spectrometer (Waters, Milford, MA, USA) was used for quantitative mass spectrometric detection as previously described [24].

2.9. Determination of kinetic parameters

Apparent K_m and V_{max} values for ovine 3βHSD towards PREG, 17-OHPREG and DHEA were determined in COS-1 cells transiently cotransfected with either ovine 3βHSD (0.5 μg) and *holo*-b_5 (0.5 μg) or ovine 3βHSD (0.5 μg) and the mammalian expression vector pCI-neo (0.5 μg) (Promega, Madison, WI, USA), which contained no DNA insert. The metabolism of PREG, 17-OHPREG and DHEA was assayed, as described in Section 2.3, using six different substrate concentrations ranging from 0.5 to 8 μM. Initial reaction rates (nmol/h/mg total protein) were determined by linear regression for each substrate and substrate concentration, using GraphPad Prism (version 5) software (GraphPad Software, San Diego, California). A minimum of four time points were used for each rate determination with the *R*-squared value for all rate regressions being higher than 0.96. Michaelis–Menten graphs for each substrate were subsequently plotted in GraphPad Prism. Apparent K_m (μM) and V_{max} values (nmol/h/mg total protein) were determined by performing Michaelis–Menten curve fits, using the non-linear regression function of the GraphPad Prism5 software. All statistical analyses were performed using GraphPad Prism (version 5) software (GraphPad Software, San Diego, California) [17,18].

2.10. Kinetic modeling

A simplified generic bi-substrate rate equation for computational systems biology [25] was used to describe the kinetics of 3βHSD during the conversion of Δ^5 steroids to their corresponding Δ^4 steroid products. The kinetic equations were cast in a system of ordinary differential equations (ODEs) that describe the rate of change of the Δ^5 steroid substrates and the Δ^4 steroid products. The system of ODEs was solved with the NDSolve function of Mathematica 6 (Wolfram Research Inc.). The constructed model was assigned arbitrary binding constant values. The initial concentration of the Δ^4 steroid product was set to 0, the NAD^+/NADH ratio was set to a fixed constant and the initial Δ^5 steroid substrate concentration was varied over a given concentration range. The model was used to determine the initial rate of conversion of the Δ^5 steroid substrates to their corresponding Δ^4 steroid products at different initial Δ^5 steroid concentrations. Following the initial simulation, a second simulation was performed in which the K_{NAD^+} value was decreased by an arbitrary value. The results obtained from these simulations were tabulated and used to construct a double-reciprocal or Lineweaver–Burke plot.

3. Results

3.1. Effect of Cyt-b_5 on 3βHSD activity in COS-1 cells

3.1.1. Caprine and ovine 3βHSD activity towards PREG, 17-OHPREG and DHEA

Caprine and ovine 3βHSD were both expressed in COS-1 cells and assayed for activity with 1 μM PREG, 17-OHPREG and DHEA as substrates. Coexpression with *holo*-b_5 resulted in a significant increase in the conversion of the three steroid substrates for both enzymes with a more pronounced difference in substrate conversion being observed at later time points (Fig. 1). In cells expressing caprine 3βHSD the addition of *holo*-b_5 resulted in a significant increase of ≈15% in the conversion of Δ^5 steroids to their corresponding Δ^4 products after 2 h (Figs. 1 and 2). In contrast, the increase in enzymatic activity of ovine 3βHSD after 2 h in the presence of *holo*-b_5 did not follow the same trend for all substrates. PREG and DHEA metabolism were significantly increased by 13.5% (±1.1 SEM) and 24% (±0.4 SEM), respectively, while the effect on 17-OHPREG conversion was minimal (5% ± 1.4 SEM) (Figs. 1 and 2).

3.1.2. Ovine 3βHSD activity towards PREG in the presence of 11βHSD2 and trunc-b_5

In order to determine whether the observed stimulation of 3βHSD activity by Cyt-b_5 was due to a non-specific membrane effect, ovine 3βHSD was coexpressed with another microsomal enzyme (11βHSD2) and assayed for activity towards PREG. The coexpression of ovine 3βHSD with human 11βHSD2 in COS-1 cells did not result in a significant change in activity when assayed with 1 μM PREG. Conversely, the inclusion of *holo*-b_5 resulted in a significant ($p < 0.01$) increase in PREG metabolism (Fig. 3).

Further investigations into non-specific membrane effects necessitated the preparation of trunc-b_5 (1–89 AA), which would not associate with the ER membrane as it does not contain the membrane spanning domain [26,27]. Ovine 3βHSD was subsequently cotransfected into COS-1 cells with trunc-b_5 and assayed for activity with 1 μM PREG. Interestingly, cotransfection with trunc-b_5 significantly ($p < 0.001$) increased the activity of ovine 3βHSD towards PREG (Fig. 3).

3.1.3. Effect of apo-b_5 on PREG metabolism

Further investigations into the augmentation of 3βHSD activity by Cyt-b_5, were carried out by cotransfecting COS-1 cells with ratios ranging from 1:1 to 1:4 of ovine 3βHSD to either *holo*-b_5 or *apo*-b_5 [28]. *Apo*-b_5, the H68A Cyt-b_5 mutant which cannot bind heme [19], was used to investigate the mechanism through which Cyt-b_5 augments 3βHSD activity.

A significant ($p < 0.01$) increase in 3βHSD activity towards PREG was observed with a concomitant increase in the ratio of 3βHSD to both *holo*-b_5 and *apo*-b_5 to (Fig. 4). The 1:4 ratio resulted in maximal stimulation for both *holo*-b_5 and *apo*-b_5 with the greatest increase in stimulation of 3βHSD activity being observed when the ratio was adjusted from 1:2 to 1:4. In addition, this increase in the stimulation of 3βHSD activity was significantly greater ($p < 0.05$) in the case of *holo*-b_5 compared to that of *apo*-b_5 (Fig. 4).

3.1.4. Comparison of 3βHSD and holo-b_5 expression levels in COS-1 cells using CFP and YFP fusion proteins

Differences in 3βHSD concentration, which may arise from variations in transfection efficiency, could result in differences in 3βHSD enzyme activity. The expression levels of 3βHSD and *holo*-b_5 following cotransfection were therefore investigated using 3βHSD-CFP and *holo*-b_5-YFP fusion proteins and the fluorescence of each protein in cells containing both fluorescent signals was subsequently analyzed. In addition, cells were cotransfected with 3βHSD-CFP and *holo*-b_5-YFP in ratios varying from 1:1 to 1:4 to determine whether varying the amount of plasmid DNA used in the transfection of the cells could alter protein expression levels.

No significant difference was observed between the fluorescent signals for 3βHSD-CFP or *holo*-b_5-YFP between the three independent cotransfection experiments (Fig. 5A). In addition, the ratio between *holo*-b_5-YFP and 3βHSD-CFP fluorescence remained constant between the different experiments (Fig. 5B). Furthermore, a significant ($p < 0.001$) increase in the fluorescent signal for *holo*-b_5-YFP was observed with a concomitant increase in the ratio of

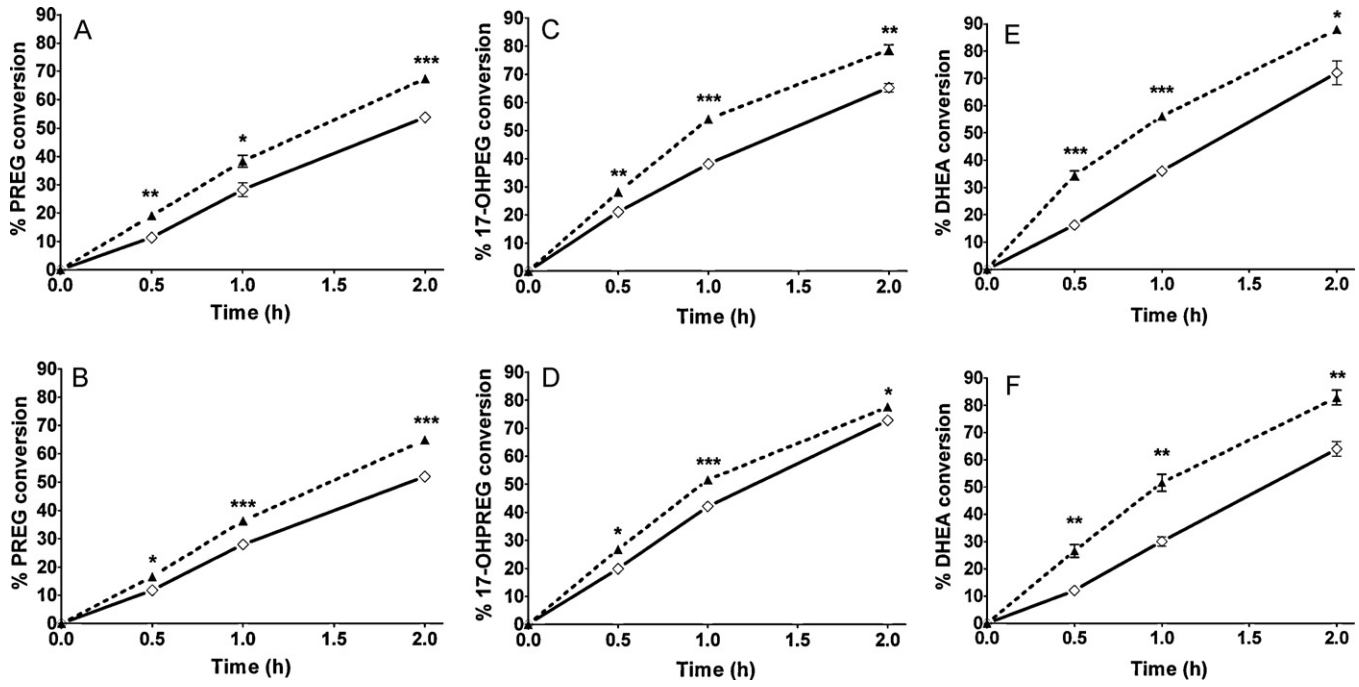

Fig. 1. Time courses of steroid metabolism by caprine and ovine 3βHSD. The conversion of 1 μM PREG, 1 μM 17-OHPREG and 1 μM DHEA by caprine (A, C and E) and ovine (B, D and F) 3βHSD was compared in the presence of either *holo*-b_5 (▲) or pCIneo (◊). Results were compared individually for each time point using an unpaired *t*-test. Results are expressed as the mean ± SEM ($^{*}p < 0.05$, $^{**}p < 0.01$, $^{***}p < 0.001$, $n = 3$).

3βHSD-CFP to *holo*-b_5-YFP, while the fluorescent signal for 3βHSD-CFP remained constant (Fig. 6).

3.1.5. Kinetic parameters of Angora and ovine 3βHSD

Apparent K_m and V_{max} values of ovine 3βHSD towards PREG, 17-OHPREG and DHEA were determined using non-linear regression in the presence and absence of *holo*-b_5. These data showed that the presence of *holo*-b_5 had no influence on the apparent K_m values while significantly ($p < 0.05$) increasing the V_{max} values towards each of the respective substrates (Table 1).

3.1.6. The influence/effect of Cyt-b_5 on co-factor binding

A simplified irreversible bi-substrate rate equation was used to construct a model in order to simulate the effect that alterations in the K_{NAD^+} value would have on the catalytic activity of 3βHSD (i.e. V_{max}) [25,29]. Results from these simulations showed that by altering the K_{NAD^+} value the V_{max} value could be manipulated without altering the K_m value (Fig. 7). Decreasing the K_{NAD^+} value resulted in an increase in the V_{max} with no effect on the K_m, which corresponds to the experimental data generated in Section 3.1.5 (Fig. 7 and Table 1).

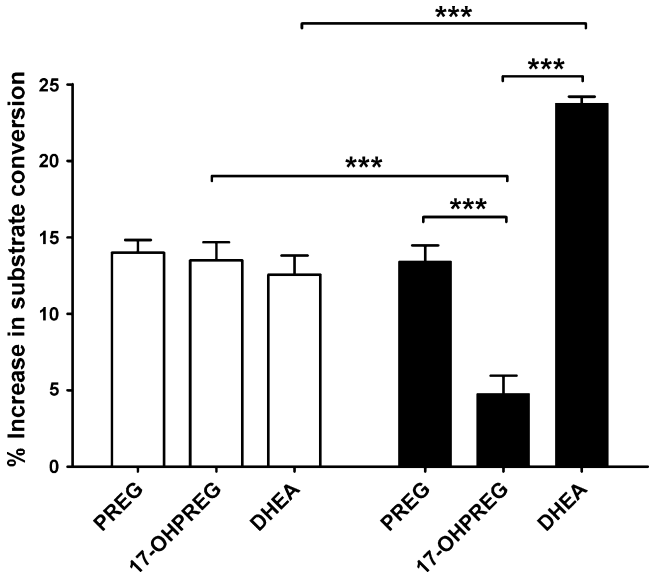

Fig. 2. Substrate conversion by 3βHSD in the presence of *holo*-b_5 in COS-1 cells. The percentage increase in substrate conversion by caprine (□) and ovine (■) 3βHSD after 2 h was compared individually using an unpaired *t*-test. Results are expressed as the mean ± SEM ($^{***}p < 0.001$, $n = 3$).

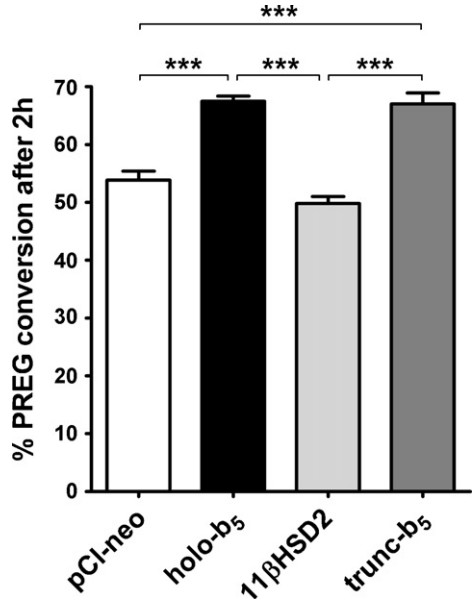

Fig. 3. Influence of *holo*-b_5, 11βHSD2 and trunc-b_5 on ovine 3βHSD cotransfected in COS-1 cells. The conversion of PREG (1 μM) was compared individually in the presence of constructs using an unpaired *t*-test. Results are expressed as the mean ± SEM ($^{***}p < 0.001$, $n = 3$).

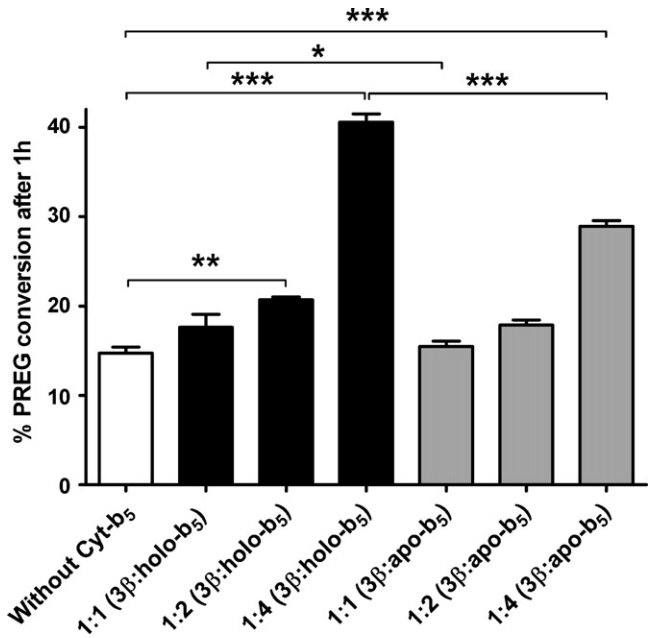

Fig. 4. Influence of *holo*- and *apo*-b_5 on substrate conversion in COS-1 cells. Cells were cotransfected with ovine 3βHSD and *holo*-b_5 or *apo*-b_5 in ratios ranging from 1:1 to 1:4. PREG (1 μM) conversion was compared individually with each ratio using an unpaired *t*-test. Results are expressed as the mean ± SEM, ($^{*}p < 0.05$, $^{**}p < 0.01$, $^{***}p < 0.001$, $n = 3$).

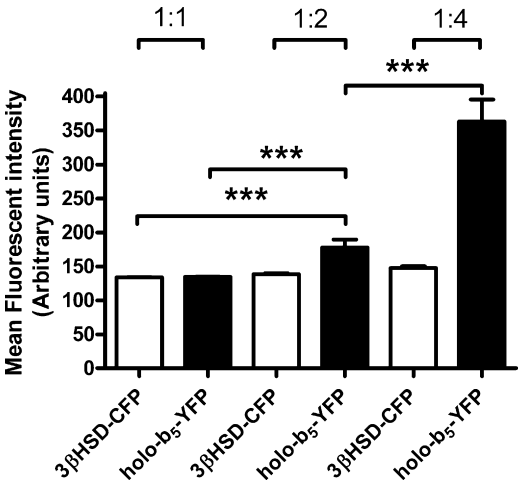

Fig. 6. Fluorescent intensity of *holo*-b_5-YFP and 3βHSD-CFP fusion proteins in COS-1 cells. Cells were cotransfected with 3βHSD-CFP and *holo*-b_5-YFP and in ratios ranging from 1:1 to 1:4. The fluorescent intensity of each fusion protein for each respective ratio was compared individually using an unpaired *t*-test. Results are expressed as the mean ± SEM ($^{***}p < 0.001$, $n = 3$).

3.2. Effects of Cyt-b_5 on 3βHSD activity in ovine adrenal microsomes

3.2.1. Microsomal 3βHSD activity towards PREG, 17-OHPREG and DHEA

The influence of purified Cyt-b_5 on 3βHSD activity was further investigated in ovine adrenal microsomes. The P450 and Cyt-b_5 concentrations in the microsomal preparation, determined spectrophotometrically [22,23], were 0.5 nmol/mg protein and 0.06 nmol/mg protein respectively. These proteins were found to be expressed at a ratio of [P450]:[Cyt-b_5] ≈ 8:1 in the adrenal microsomes, which correlated with previous results obtained by Swart et al. [10] who showed the presence of low levels of endogenous Cyt-b_5 in ovine adrenal microsomes.

Ovine adrenal microsomes (0.35 μM P450) were assayed for 3βHSD activity towards PREG (10 μM), 17-OHPREG (20 μM) and DHEA (20 μM). The addition of purified Cyt-b_5 (0.4 μM), which represents a 10-fold increase in Cyt-b_5 concentration (relative to endogenous Cyt-b_5), resulted in a significant ($p < 0.01$) increase in PREG (10.3% ± 0.3 SEM) and DHEA (7.6% ± 0.2 SEM) conversion (Fig. 8A and C), while having no effect on 17-OHPREG conversion (Fig. 8B). The addition of trilostane (10 μM), a known 3βHSD specific inhibitor, abolished 3βHSD activity towards the three substrates (results not shown), confirming that the observed activity was specific for 3βHSD.

In addition to the incubation of the microsomal preparation with purified Cyt-b_5, the preparation was also incubated with anti-Cyt-b_5 IgG in order to determine the effect of endogenous Cyt-b_5 on microsomal 3βHSD activity. The microsomal preparation was incubated with purified anti-Cyt-b_5 IgG, previously raised in our laboratory [10], and assayed for activity with 10 μM PREG and 20 μM DHEA, as substrates. The addition of purified anti-Cyt-b_5 IgG significantly ($p < 0.05$) reduced 3βHSD activity towards PREG, while the addition of anti-HRP (horse radish peroxidase) IgG (control), had no effect on activity (Fig. 9A). A similar trend was observed for the metabolism of DHEA in the presence of purified anti-Cyt-b_5 IgG, however, the reduction in activity was not statistically significant (Fig. 9B).

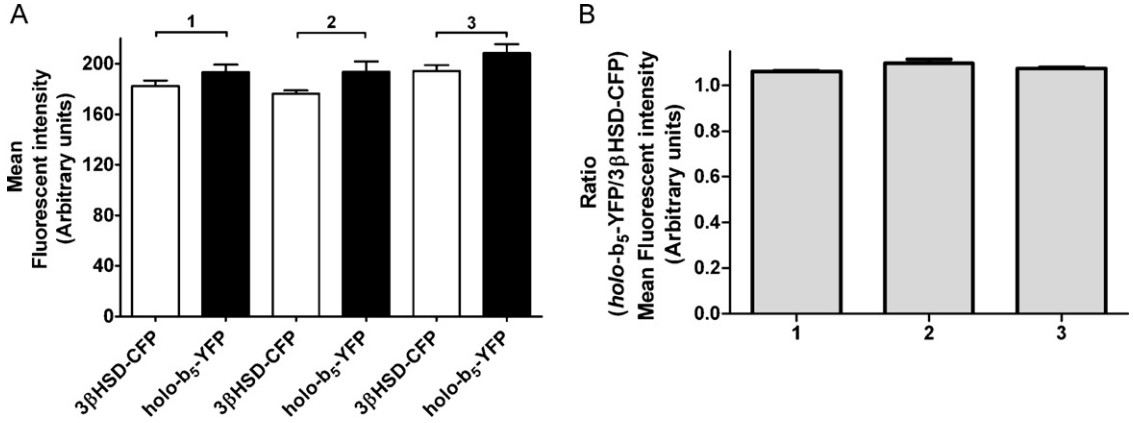

Fig. 5. The fluorescent intensity of 3βHSD-CFP and *holo*-b_5-YFP fusion proteins expressed in COS-1 cells. (A) The mean fluorescent intensity in three independent cotransfection experiments and (B) the ratio between the fluorescent intensity in three independent cotransfection experiments. The fluorescent intensities were compared using a one-way ANOVA followed by Bonferroni's multiple comparison post-test. Results are expressed as the mean ± SEM ($n = 3$).

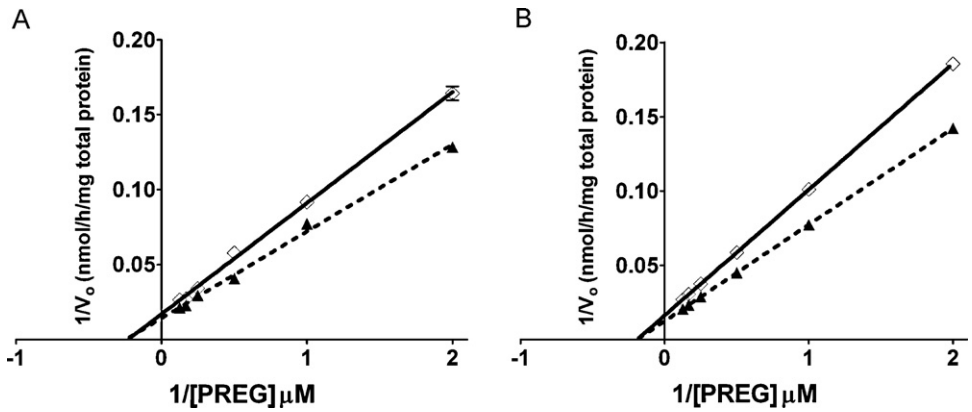

Fig. 7. Effect of Cyt-b_5 and varying K_{NAD^+} values on the kinetics of ovine 3βHSD in the conversion of PREG. (A) Comparison of ovine 3βHSD kinetics in the presence (▲) and absence (◊) of Cyt-b_5, determined experimentally. (B) Comparison of ovine 3βHSD kinetics, as predicted by the theoretical model, incorporating either high (◊) or low (▲) K_{NAD^+} values.

Table 1
Apparent K_m and the V_{max} values of ovine 3βHSD towards PREG, 17-OHPREG and DHEA in the presence and absence of *holo*-b_5. Apparent K_m (μM) and the V_{max} values (nmol/h/mg protein) were determined as described in Section 2.9 and are expressed as the mean ± SEM. The apparent K_m and V_{max} values of ovine 3βHSD are compared independently to that of ovine 3βHSD plus *holo*-b_5 for each substrate using an unpaired *t*-test.

Ovine 3βHSD	PREG		17-OHPREG		DHEA	
	K_m	V_{max}	K_m	V_{max}	K_m	V_{max}
– *holo*-b_5	4.7 ± 0.5	63.3 ± 3.6	0.9 ± 0.2	101.6 ± 4.6	1.8 ± 0.2	22.4 ± 1.7
+ *holo*-b_5	4.3^{ns} ± 0.4	73.6^{*} ± 3.8	1.2^{ns} ± 0.4	124.8^{**} ± 4.4	1.7^{ns} ± 0.3	172.1^{***} ± 8.2

$^{ns}p > 0.05$.
$^{*}p < 0.05$.
$^{**}p < 0.01$.
$^{***}p < 0.001$.
$n = 3$.

3.2.2. *Effect of increased Cyt-b_5 concentrations on microsomal 3βHSD activity*

3βHSD activity was assayed using 10 μM PREG in ovine adrenal microsomes (0.35 μM P450; 0.04 μM endogenous Cyt-b_5) which were incubated in the presence of 0.04–44 μM Cyt-b_5 added in ratios ranging from 1:1 to 1:100 of endogenous Cyt-b_5 to added Cyt-b_5. A distinct increase in the conversion of PREG was observed in conjunction with an increase in the ratio of endogenous Cyt-b_5 to added Cyt-b_5. Maximal stimulation was observed at a ratio of 1:10. Increasing the ratio above 1:10 resulted in a significant ($p < 0.01$) decrease in the observed stimulation, with the 1:100 ratio showing no observable effect on PREG metabolism (Fig. 10).

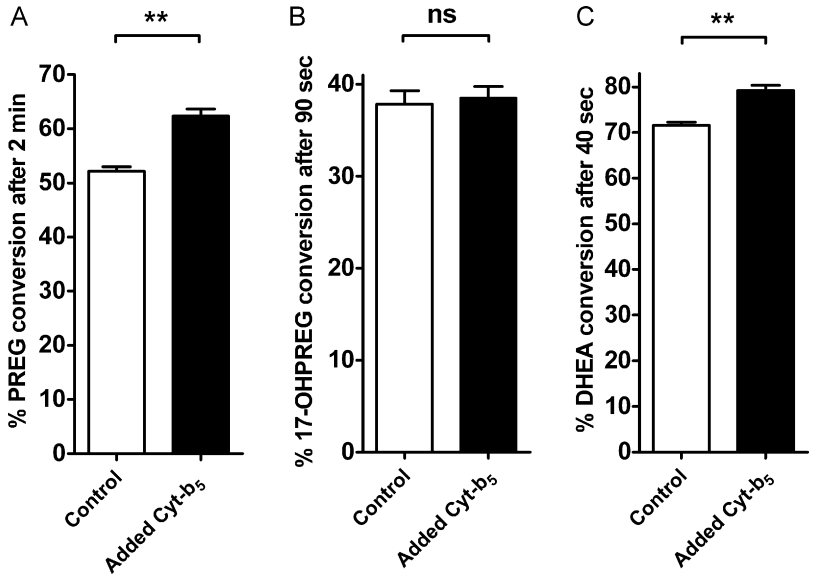

Fig. 8. Influence of added Cyt-b_5 on substrate conversion in ovine adrenal microsomes. (A) PREG, 10 μM; P450, 0.35 μM; endogenous Cyt-b_5, 0.04 μM; added Cyt-b_5, 0.4 μM; (B) 17-OHPREG, 20 μM; P450, 0.35 μM; endogenous Cyt-b_5, 0.04 μM; added Cyt-b_5, 0.4 μM and (C) DHEA, 20 μM; P450, 0.17 μM; endogenous Cyt-b_5, 0.02 μM; added Cyt-b_5, 0.2 μM. Substrate conversion was compared individually for each substrate in the presence/absence of purified Cyt-b_5 using an unpaired *t*-test. Results are expressed as the mean ± SEM ($^{ns}p > 0.05$, $^{**}p < 0.01$, $n = 3$).

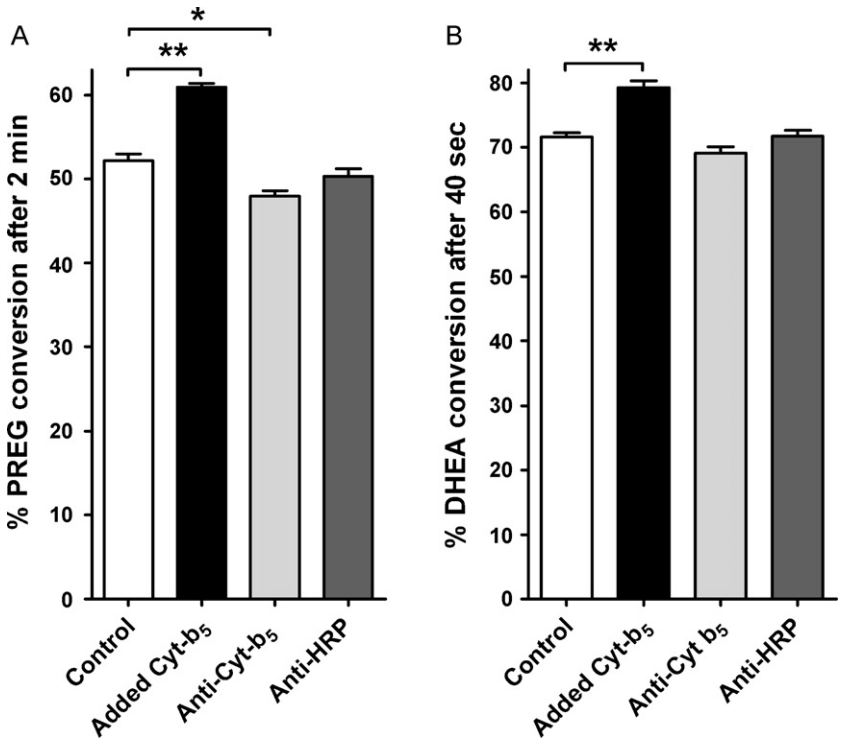

Fig. 9. Influence of anti-Cyt-b_5 IgG on substrate conversion in ovine adrenal microsomes. (A) PREG, 10 μM; P450, 0.35 μM; endogenous Cyt-b_5, 0.04 μM; added Cyt-b_5, 0.4 μM. (B). DHEA, 20 μM; P450, 0.17 μM; endogenous Cyt-b_5, 0.02 μM; added Cyt-b_5, 0.2 μM. Percentage conversion was compared individually for each substrate using an unpaired *t*-test. Results are expressed as the mean ± SEM ($^*p < 0.05$, $^{**}p < 0.01$, $n = 3$).

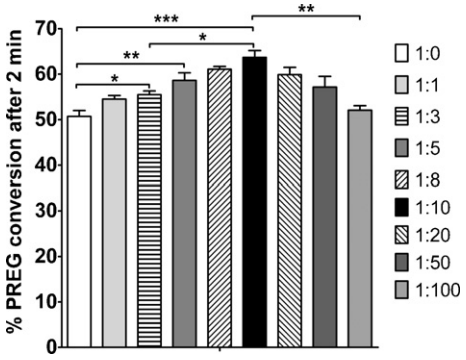

Fig. 10. PREG conversion in the presence of added Cyt-b_5 in ovine adrenal microsomes. PREG, 10 μM; P450, 0.35 μM; endogenous Cyt-b_5, 0.04 μM; ratios of endogenous Cyt-b_5:added Cyt-b_5, 1:0–1:100. PREG conversion was compared individually using an unpaired *t*-test. Results are expressed as the mean ± SEM ($^*p < 0.05$, $^{**}p < 0.01$, $^{***}p < 0.001$, $n = 3$).

4. Discussion

In this study we showed Cyt-b_5, coexpressed with either caprine or ovine 3βHSD in COS-1 cells, significantly increased the conversion of PREG, 17-OHPREG and DHEA to their respective Δ^4 products (Fig. 1). These data suggest that, in addition to its reported role in stimulating the lyase activity of CYP17A1, Cyt-b_5 may also augment 3βHSD activity. The degree of stimulation was, however, different between the two species and between the respective steroid substrates (Fig. 2), indicating that Cyt-b_5 augmentation occurs in a species and substrate specific manner.

Augmentation of 3βHSD activity by Cyt-b_5 was subsequently shown not to be attributed to non-specific membrane effects. The coexpression of 3βHSD with 11βHSD2 (localized to ER membrane) had no effect on 3βHSD activity (Fig. 3) while trunc-b_5 (cytosolic) stimulated ovine 3βHSD activity to the same extent as *holo*-b_5 (Fig. 3). Coexpression of Cyt-b_5 with 3βHSD therefore does not alter the ER membrane environment to such an extent that 3βHSD becomes more accessible to steroid substrates and co-factors. Subsequent incubations of the microsomal preparations with anti-Cyt-b_5 IgG resulted in a significant reduction in 3βHSD activity towards PREG (Fig. 9A), confirming Cyt-b_5′s augmentation of 3βHSD. Although a similar trend was observed for DHEA metabolism, the reduction in activity by the addition of purified anti-Cyt-b_5 IgG was not statistically significant (Fig. 9B). This may be attributed to the conversion rate of DHEA with more than 70% A4 formation after 40 s even though the reaction conditions were optimized, implying that the reaction rate may no longer be linear, thus reducing the observable effect of the anti-Cyt-b_5 IgG.

The addition of purified Cyt-b_5 to microsomal preparations significantly increased 3βHSD activity towards PREG with maximum stimulation at 1:10 (endogenous Cyt-b_5:added Cyt-b_5). However, as the ratio was adjusted beyond the optimum of 1:10 the degree of stimulation was significantly reduced (Fig. 10). This was previously observed in the stimulation of CYP17A1 activity by Cyt-b_5. Auchus et al. [30] and Soucy and Luu-The [28] reported that the stimulated lyase activity was substantially reduced in the presence of excess Cyt-b_5 and concluded that this was due to electron scavenging by Cyt-b_5 from POR at higher ratios of Cyt-b_5. However, since 3βHSD does not require electrons from an external electron donor to perform its catalytic function, this seems an unlikely explanation for the reduced stimulation.

The addition of purified Cyt-b_5 had no significant effect on 17-OHPREG conversion (Fig. 8B). These results correlate with the results obtained in COS-1 cells where the greatest increase in substrate conversion by ovine 3βHSD in the presence of Cyt-b_5 was observed for PREG and DHEA, with a comparatively small increase observed for 17-OHPREG conversion (Figs. 1 and 2). The apparent V_{max} value of ovine 3βHSD towards 17-OHPREG in the absence of Cyt-b_5 is significantly greater than that of the enzyme towards PREG or DHEA (Table 1). The lack of apparent 3βHSD stimulation

by Cyt-b_5 in the conversion of 17-OHPREG could be attributed to the activity of 3βHSD towards 17-OHPREG already being high, and thus the degree to which the enzyme may be stimulated is reduced.

Traditionally, Cyt-b_5 is believed to augment the activity of specific cytochromes P450 via direct electron transfer. However, Auchus et al. [30] demonstrated that *apo*-b_5 was able to stimulate the 17,20 lyase activity of CYP17A1 and proposed an allosteric mechanism. Cyt-b_5 also plays an allosteric role in the catalysis of various other cytochrome P450 enzymes which include CYP3A4, CYP3A5 and CYP2A6 [31,32]. Guryev et al. [19], however, suggested that the stimulatory effect of *apo*-b_5 on CYP17A1 and CYP3A4 was due to the transfer of excess heme to *apo*-b_5 generating *holo*-b_5, resulting in the stimulatory effects observed. Unlike the cytochromes P450, 3βHSD does not require the input of electrons from an external electron donor and it is therefore unlikely that electron transfer plays a role. We demonstrated that *apo*-b_5 stimulated the activity of 3βHSD (Fig. 4), albeit to a lesser degree than *holo*-b_5, implying that Cyt-b_5 exerts an allosteric effect on 3βHSD. The lower stimulatory effect of *apo*-b_5 is likely due to conformational changes in the protein resulting from the removal of the heme moiety [33,34].

The kinetic constants (K_m and V_{max}) of ovine 3βHSD revealed that Cyt-b_5 had no influence on the apparent K_m values, but significantly ($p < 0.05$) increased the V_{max} values towards each of the Δ^5 substrates (Table 1). Unlike the K_m values, which are not dependent on enzyme concentration, the V_{max} values may vary as a result of differing transfection efficiencies. We previously demonstrated, using quantitative real-time PCR, that transient transfections of caprine or ovine 3βHSD in COS-1 cells consistently yield comparable mRNA levels [18]. In addition, we now show that the level of fluorescence for both the 3βHSD-CFP and *holo*-b_5-YFP fusion proteins, as well as the ratio between the two, remained relatively constant following three independent experiments (Fig. 5). Similar levels of 3βHSD and *holo*-b_5 are thus present, suggesting that it is unlikely that variations in the expression levels are responsible for the differences observed in 3βHSD activity. Furthermore, this confirms that the cotransfection of 3βHSD and *holo*-b_5 results in the expression of both enzymes in the same cell. In addition, the level of *holo*-b_5-YFP fluorescence was found to increase significantly ($p < 0.001$) as the ratio of 3βHSD-CFP:*holo*-b_5-YFP plasmid DNA used for transfection was adjusted from 1:1 to 1:4, while the level of 3βHSD-CFP fluorescence remained constant in these cells (Fig. 6). These results correlate with data presented in Fig. 4 where a relatively small increase in 3βHSD activity was observed when the ratio of *holo*-b_5:3βHSD was adjusted to 1:2. However, a greater increase in 3βHSD activity was observed with the increased ratio of 1:4. Similarly, in Fig. 6, a relatively small increase in the level of *holo*-b_5-YFP fluorescence was observed when the ratio of 3βHSD-CFP:*holo*-b_5-YFP was adjusted to 1:2 while a significantly greater increase was observed at 1:4. These results suggest that an increase in plasmid DNA can increase the level of *holo*-b_5 expressed in COS-1 cells, resulting in an increase in the level of 3βHSD stimulation, as observed in Fig. 4.

While the unchanged apparent K_m values for the steroid substrates indicate that significant conformational changes of the active site are unlikely, subtle changes brought about by the putative allosteric interactions between Cyt-b_5 and 3βHSD, may impact on co-factor binding. It is possible that the binding of NAD^+ may, be affected resulting in the stimulation of the dehydrogenase activity without influencing substrate affinity. Using a simplified irreversible bi-substrate rate equation we demonstrated that decreasing the K_{NAD^+} value results in an increase in the V_{max} value without altering the K_m value, corresponding to the experimental data (Fig. 7). Increasing the rate of the dehydrogenase reaction would lead to an increase in the overall rate of the enzyme as the isomerase activity has been shown to be ≈10-fold greater than the dehydrogenase activity [35–37]. The data generated by these simulations, in conjunction with the experimental data, thus strongly suggests that an allosteric interaction between 3βHSD and Cyt-b_5 results in an increase in the affinity of 3βHSD for NAD^+, stimulating the dehydrogenase reaction, resulting in an increase in the overall catalytic activity.

The biosynthesis of A4, a vital precursor of sex steroids, requires the coexpression of Cyt-b_5, 3βHSD and CYP17A1 [38]. While significant levels of circulating A4 are believed to originate in the adrenal cortex [39–41] the expression of 3βHSD is low in the zona reticularis (ZR), which specifically expresses Cyt-b_5. Conversely, 3βHSD is expressed in the zona fasciculate (ZF) and zona glomerulosa (ZG) in the absence of significant Cyt-b_5 expression [42,43]. Nakamura et al. [44] recently highlighted the importance of Cyt-b_5 and 3βHSD coexpression in the production of A4 and identified a layer of adrenocortical cells located at the border between the ZF and ZR that coexpress both 3βHSD and Cyt-b_5 in the presence of CYP17A1. Until now, Cyt-b_5 was only thought to play a role in the stimulation of the 17, 20-lyase reaction catalyzed by CY17A1, however, based on the results presented in this paper we suggest that Cyt-b_5 may also stimulate 3βHSD activity, thereby promoting the formation of A4 from DHEA.

In addition to the adrenal cells described above, 3βHSD and Cyt-b_5 are coexpressed in other prominent steroidogenic organs such as the kidneys, testis (Leydig cells) and ovaries (theca cells) [2,43,45,46], suggesting that Cyt-b_5 may play a more extensive role in steroidogenic reactions than originally thought. The augmentation of 3βHSD activity by Cyt-b_5 presented in this paper can, therefore not be ignored. Future studies will reveal the full physiological impact of such an augmentation.

5. Conclusions

The data presented in this study provides clear evidence that 3βHSD activity is specifically augmented by Cyt-b_5. This augmentation was further also shown to differ between closely related species and between substrates, suggesting augmentation occurs in a substrate and species specific manner. Furthermore, the data suggests that this augmentation is most likely allosteric in nature, resulting in a decreased K_{NAD^+} value leading to an overall increase in enzymatic activity.

Acknowledgments

The authors wish to thank Christina Moraal and Ruenda Odendaal – technical assistance in the preparation of anti-ovine Cyt-b_5 IgG and anti-HRP IgG. The pCR3 plasmid containing 11βHSD2 was a generous gift from Paul M. Stewart, University of Birmingham, School of Clinical and Experimental Medicine, Birmingham, United Kingdom. The Cer-5-Ven plasmid containing both CFP and YFP was a generous gift from Ammasi Periasamy, W.M. Keck Center for Cellular Imaging, Department of Biology, University of Virginia, Charlottesville, Virginia, USA. This work was financially supported by the NRF, The Harry Crossly Foundation and the University of Stellenbosch.

References

[1] T.M. Penning, Molecular endocrinology of hydroxysteroid dehydrogenases, Endocr. Rev. 18 (1997) 281–305.
[2] J. Simard, M.L. Ricketts, S. Gingras, P. Soucy, F.A. Feltus, M.H. Melner, Molecular biology of the 3β-hydroxysteroid dehydrogenase/Δ5-Δ4 isomerase gene family, Endocr. Rev. 26 (2005) 525–582.
[3] L. Van, T. Masakazu, Y. de Launoit, M. Dumont, Y. Lachance, F. Labrie, Evidence for distinct dehydrogenase and isomerase sites within a single 3β-hydroxysteroid dehydrogenase/5-ene-4-ene isomerase protein, Biochemistry 36 (1991) 8861–8865.

[4] J.L. Thomas, C. Frieden, W.E. Nash, R.C. Strickler, An NADH-induced conformational change that mediates the sequential 3β-hydroxysteroid dehydrogenase/isomerase activities is supported by affinity labeling and time-dependent activation of isomerase, J. Biol. Chem. 270 (1995) 21003–21008.
[5] J.L. Thomas, W.L. Duax, A. Addlagatta, S. Brandt, R.R. Fuller, W. Norris, Structure/function relationships responsible for coenzyme specificity and the isomerase activity of human type 1 3β-hydroxysteroid dehydrogenase/isomerase, J. Biol. Chem. 278 (2003) 35483–35490.
[6] S. Nakajin, P.F. Hall, Microsomal cytochrome P-450 from neonatal pig testis. Purification and properties of A C21 steroid side chain cleavage system (17α hydroxylase-C17,20 lyase), J. Biol. Chem. 256 (1981) 3871–3876.
[7] S. Nakajin, J.E. Shively, P. Yuan, P.F. Hall, Microsomal cytochrome P450 from neonatal pig testis: two enzymatic activities (17α-hydroxylase and C17,20-lyase) associated with one protein, Biochemistry 20 (1981) 4037–4042.
[8] M.X. Zuber, E.R. Simpson, M.R. Waterman, Expression of bovine 17α-hydroxylase cytochrome P-450 *c*DNA in nonsteroidogenic (COS-1) cells, Science 234 (1986) 1258–1261.
[9] A.J. Conley, I.M. Bird, The role of cytochrome P450 17α-hydroxylase and 3β-hydroxysteroid dehydrogenase in the integration of gonadal and adrenal steroidogenesis via the Δ5 and Δ4 pathways of steroidogenesis in mammals, Biol. Reprod. 56 (1997) 789–799.
[10] P. Swart, N. Lombard, A.C. Swart, T. van der Merwe, B.A. Murry, M. Nicol, J.I. Mason, Ovine steroid 17α-hydroxlyase cytochrome P450: characteristics of the hydroxylase and lyase activities of the adrenal cortex enzymes, Arch. Biochem. Biophys. 409 (2003) 145–152.
[11] A.H. Payne, D.B. Hales, Overview of steroidogenic enzymes in the pathway from cholesterol to active steroid hormones, Endocr. Rev. 25 (2004) 947–970.
[12] W.E. Rainey, Y. Nakamura, Regulation of the adrenal androgen biosynthesis, J. Steroid Biochem. Mol. Biol. 108 (2008) 281–286.
[13] M. Katagiri, K. Suhara, M. Shiroo, Y. Fujimura, Role of cytochrome b_5 in the cytochrome P-450-mediated C21-steroid 17,20-lyase reaction, Biochem. Biophys. Res. Commun. 108 (1982) 379–384.
[14] M. Katagiri, N. Kagawa, M.R. Waterman, The role of cytochrome b_5 in the biosynthesis of androgens by human P450c17, Arch. Biochem. Biophys. 317 (1995) 343–347.
[15] F.S. Mathews, The structure, function and evolution of cytochromes, Prog. Biophys. Mol. Biol. 45 (1985) 1–56.
[16] J.B. Schenkman, I. Jansson, The many roles of cytochrome b_5, Pharmacol. Ther. 97 (2003) 139–152.
[17] K-H. Storbeck, A.C. Swart, J.T. Slabbert, P. Swart, The identification of two CYP17 alleles in the South African Angora goat, Drug Metab. Rev. 39 (2007) 1–14.
[18] P. Goosen, A.C. Swart, K.H. Storbeck, P. Swart, Hypocortisolism in the South African Angora goat: the role of 3βHSD, Mol. Cell. Endocrinol. 315 (2010) 182–187.
[19] O.L. Guryev, A.A. Gilep, S.A. Usanov, R.W. Estabrook, Interaction of Apocytochrome b_5 with cytochromes P4503A4 and P45017A: relevance of heme transfer reactions, Biochemistry 40 (2001) 5018–5031.
[20] P.M. Stewart, C.B. Whorwood, 11β-Hydroxysteroid dehydrogenase activity and corticosteroid hormone action, Steroids 59 (1994) 90–95.
[21] M-X. Yang, A.I. Cederbaum, Fractionation of liver microsomes with polyethylene glycol and purification of NADH-cytochrome b_5 oxidoreductase and cytochrome b_5, Arch. Biochem. Biophys. 315 (1994) 438–444.
[22] T. Omura, R. Sato, The carbon monoxide-binding pigment of liver microsomes, J. Biol. Chem. 239 (1964) 2379–2385.
[23] R.W. Estabrook, J. Werringloer, The measurement of difference spectra: application to cytochromes of microsomes, Methods Enzymol. 52 (1978) 212–220.
[24] K-H. Storbeck, N.W. Kolar, M. Stander, A.C. Swart, D. Prevoo, P. Swart, The development of an ultra performance liquid chromatography-coupled atmospheric pressure chemical ionization mass spectrometry assay for seven adrenal steroids, Anal. Biochem. 372 (2008) 11–20.
[25] J.M. Rohwer, A.J. Hanekom, C. Crous, J.L. Snoep, J.-H.S. Hofmeyer, Evaluation of a simplified generic bi-substrate rate equation for computational systems biology, IEE Proc.-Syst. Biol. 153 (2006) 338–341.
[26] L. Spatz, P. Strittmatter, A form of cytochrome b_5 that contains an additional hydrophobic sequence of 40 amino acid residues, Proc. Natl. Acad. Sci. U. S. A. 68 (1971) 1042–1046.
[27] M.P.A. Henderson, Y.T. Hwang, J.M. Dyer, R.T. Mullen, D.A. Andrews, The C-terminus of cytochrome b_5 confers endoplasmic reticulum specificity by preventing spontaneous insertion into membranes, Biochem. J. 401 (2007) 701–709.
[28] P. Soucy, V. Luu-The, Assessment of the ability of type 2 cytochrome b_5 to modulate 17,20-lyase activity of human P450c17, J. Steroid Biochem. Mol. Biol. 80 (2002) 71–75.
[29] K-H. Storbeck, P. Swart, D. Africander, R. Conradie, R. Louw, A.C. Swart, 16α-Hydroxyprogesterone: origin, biosynthesis and receptor interaction, Mol. Cell. Endocrinol. 336 (2010) 92–101.
[30] R.J. Auchus, T.C. Lee, W.L. Miller, Cytochrome b_5 augments the 17,20-lyase activity of human P450c17 without direct electron transfer, J. Biol. Chem. 273 (1998) 3158–3165.
[31] H. Yamazaki, W.W. Johnson, Y.F. Ueng, T. Shimada, F.P. Guengerich, Lack of electron transfer from cytochrome b_5 in stimulation of catalytic activities of cytochrome P450 3A4. Characterization of a reconstituted cytochrome P450 3A4/NADPH-cytochrome P450 reductase system and studies with apocytochrome b_5, J. Biol. Chem. 271 (1996) 27438–27444.
[32] H. Yamazaki, M. Nakamura, T. Komatsu, K. Ohyama, N. Hatanaka, S. Asahi, N. Shimada, F.P. Geungerich, T. Shimada, M. Nakajima, T. Yokoi, Roles of NADPH-P450 reductase and apo- and holo-cytochrome b_5 on xenobiotic oxidations catalyzed by 12 recombinant human cytochrome P450s expressed in membranes of *Escherichia coli*, Protein Expr. Purif. 24 (2002) 329–337.
[33] W. Pfeil, Thermodynamics of apocytochrome b_5 unfolding, Protein Sci. 2 (1993) 1497–1501.
[34] E.M. Storch, V. Daggett, Structural consequences of heme removal: molecular dynamics simulations of rat and bovine apocytochrome b_5, Biochemistry 35 (1996) 11596–11604.
[35] J.L. Thomas, E.A. Berko, A. Faustino, R.P. Myers, R.C. Strickler, Human placental 3β-hydroxy-5-ene-steroid dehydrogenase and steroid 5 → 4-ene-isomerase: purification from microsomes, substrate kinetics and inhibition by product steroids, J. Steroid Biochem. 31 (1988) 785–793.
[36] J.L. Thomas, R.P. Myers, R.C. Strickler, Human placental 3β-hydroxy-5-ene-steroid dehydrogenase and steroid 5 → 4-ene-isomerase: purification from mitochondria and kinetic profiles, biophysical characterization of the purified mitochondrial and microsomal enzymes, J. Steroid Biochem. 33 (1989) 209–217.
[37] W.E. Nash, R.W. Mercer, G. Blanco, R.C. Strickler, J.I. Mason, J.L. Thomas, Over-expression of human type I (placental) 3β-hydroxy-5-ene-steroid dehydrogenase/isomerase in insect cells infected with recombinant baculovirus, J. Steroid Biochem. Mol. Biol. 50 (1994) 235–240.
[38] C.E. Flück, W.L. Miller, R.J. Auchus, 17,20-Lyase activity of cytochrome p450c17 from human fetal testis favors the delta5 steroidogenic pathway, J. Clin. Endocrinol. Metab. 88 (2003) 3762–3766.
[39] E.I. Georgiadis, C. Matzoros, C. Aliferis, M. Batrinos, Are adrenal and testicular androgen levels correlated? Horm. Metab. Res. 24 (1992) 488–491.
[40] H.G. Burger, Androgen production in women, Fertil. Steril. 77 (2002) S3–S5.
[41] T. Piltonen, R. Koivunen, L. Morin-Papunen, A. Ruokonen, I.T. Huhtaniemi, J.S. Tapanainen, Ovarian and adrenal steroid production: regulatory role of LH/HCG, Hum. Reprod. 17 (2002) 620–624.
[42] T. Suzuki, H. Sasano, J. Takeyama, C. Kaneko, W.A. Freije, B.R. Carr, W.E. Rainey, Developmental changes in steroidogenic enzymes in human postnatal adrenal cortex: immunohistochemical studies, Clin. Endocrinol. 53 (2000) 739–747.
[43] S. Dharia, A. Slane, M. Jian, M. Conner, A.J. Conley, C.R. Parker Jr., Colocalization of P450c17 and cytochrome b5 in androgen-synthesizing tissues of the human, Biol. Reprod. 71 (2004) 83–88.
[44] Y. Nakamura, Y. Xing, X-G. Hui, Y. Kurotaki, K. Ono, T. Cohen, H. Sasano, W.E. Rainey, Human adrenal cells that express both 3β-hydroxysteroid dehydrogenase type 2 (HSD3B2) and cytochrome b5 (CYB5A) contribute to adrenal androstenedione production, J. Steroid Biochem. Mol. Biol. 123 (2011) 122–126.
[45] E. Rheaume, Y. Lachance, H.F. Zhao, N. Breton, M. Dumont, Y. de Launoit, C. Trudel, V. Luu-The, J. Simard, F. Labrie, Structure and expression of a new complementary DNA encoding the almost exclusive 3β-hydroxysteroid dehydrogenase/Δ5-Δ4 isomerase in human adrenals and gonads, Mol. Endocrinol. 5 (1991) 1147–1157.
[46] M. Quinkler, C. Bumke-Vogt, B. Meyer, V. Bahr, W. Oelkers, S. Diederich, The human kidney is a progesterone-metabolizing and androgen-producing organ, J. Clin. Endocrinol. Metab. 88 (2003) 2803–2809.